INTECH
open science | open minds

OPEN ACCESS
ARTICLE

Nanomaterials and Nanotechnology

Sonication-Assisted Synthesis of β-Mercuric Sulphide Nanoparticles

Regular Paper

Xin Xu[1,2] and Elizabeth R. Carraway[1,*]

1 Department of Environmental Engineering & Earth Sciences, Clemson University, Anderson, SC, USA
2 Present address: Civil Engineering Room T-182, Department of Civil Engineering, Steinman Hall, The City College of New York, New York, NY, USA
* Corresponding author E-mail: ecarraw@clemson.edu

Received 2 November 2012; Accepted 15 December 2012

Abstract The nanoscale semiconductor β-mercuric sulphide (HgS) has promising applications in electronic and optical fields. Continued development of synthesis methods is needed to expand approaches that produce uniform particles, while avoiding reagents of high toxicity and ecological impact. A solvent-based approach was developed using mercuric chloride and elemental sulphur as the mercury and chalcogenide sources. Ethanol was used as the solvent and sodium hydroxide as the hydrolysis reagent. Use of mild sonication resulted in smaller particles (average 11nm diameter) than without sonication treatment (average 17nm diameter) and continuous nitrogen purging reduced the surface oxygen content of the particles from approximately 25% to 6%. Particle characterization methods included TEM, XRD, XPS, UV-visible absorbance spectroscopy and DLS. The nanoparticles were typically spheres of 10-15nm in diameter. Aggregates formed in aqueous solutions tended to be in the range of 100nm or more. The overall process can be performed simply at room temperature and is comparatively free of toxic chemical hazards. The process does not include surfactants or other stabilizers that could potentially contaminate the nanocrystals. In principle, the method could be applied to synthesis of other metal chalcogenide nanoparticles.

Keywords Metacinnabar, Base Hydrolysis, Colloids, Mercuric Salts, Ethanol, Elemental Sulphur

1. Introduction

Mercuric sulphide (HgS) is widely used in acousto-optical materials [1], infrared sensing [2] and photoelectronic applications [3-5]. Two different HgS crystal structures, α-HgS (cinnabar, trigonal type, hexagonal) and β-HgS (metacinnabar, zinc-blende type, cubic) have been intensively explored. Metacinnabar, a strong topological insulator, is a unique material, which can be used for low-power consumption electronic devices [6]. As particle sizes decrease to a nanometre scale, quantum confinement effects and large surface to volume ratios make these applications even more significant. In particular, nano-sized HgS has a potential use in solid state solar cells and photoelectrochemical cells [5]. Thus, developments in its synthesis methods are of continuing interest. Nanoparticles (NPs) are naturally ubiquitous in the environment and are formed by processes that have occurred for millions of years. Submicron crystalline HgS in the form of metacinnabar was detected in mercury-contaminated soil from the

flood plain of the East Fork Poplar Creek in Oak Ridge, Tennessee [7]. Nanocolloidal metacinnabar was produced in mercury-NOM-sulphide systems in a synthetic natural environment [8]. NOM, especially low molecular weight thiol-containing organic acids, hindered the precipitation, aggregation and further grow of nanoHgS [9]. In addition, there is evidence that nanoHgS will increase mercury methylation in the presence of NOM [10, 11]. Research on the applications and environmental behaviour of NPs such as β-HgS requires materials in a variety of forms, from high purity to particles of controlled size and shape with stabilizing surface modifications.

Practical and facile methods to synthesize nano-sized β-HgS particles remain a challenge. Established methods include chemical deposition [12], solvothermal [13-14], microwave heating [15-17], photochemical [18], wet chemical [19] and electrochemical [20]. A common difficulty is the aggregation of irregularly shaped particles with a wide size distribution. Particle morphology is difficult to control in methods conducted at ambient temperatures and results in large irregular particles. Thus, surfactants and organic solvents, including formaldehyde [15], triethylene tetratamine [13], polyvinyl alcohol [19] and ethylenediamine [21] have been introduced to synthesis procedures. Although surfactants can assist in dispersing the nanoparticles, contamination of the final material may occur, affecting chemical and toxicological behaviour. Avoiding toxic and/or specialty chemicals such as hydrogen sulphide and organomercury compounds during synthesis is also a concern. Thus, continued development of synthesis methods is needed to generate particles with a range of properties and to reduce synthesis hazards and ecological impacts.

The present work uses a solvent based approach for the synthesis of β-HgS nanocrystals. The synthesis is carried out following sonication and nitrogen purging at an ambient temperature. Surfactants and stabilizing ligands were not used in order to avoid affecting chemical and toxicological behaviour in subsequent studies of the NPs. The structural and optical properties of β-HgS were measured by transmission electron microscopy (TEM), X-ray diffraction (XRD), X-ray photoelectron spectroscopy (XPS), dynamic light scattering (DLS) and UV-visible (UV-vis) absorbance spectroscopy.

2. Experimental section

2.1 Materials and synthesis procedure

All chemicals were reagent grade or higher and were used without further purification. Reagents included mercuric chloride ($HgCl_2$) and sulphur from Alfa Aesar, sodium hydroxide (NaOH) and ethanol (94-96% denatured with methanol and 2-propanol) from Mallinckrodt and pentane and hexane (HPLC grade) from Burdick and Jackson. High purity nitrogen gas (99.9989%) and Type I ultrapure water (Milli-Q System, ≥16 MΩ·cm) were also used.

A solution of 1.0g $HgCl_2$ in 50mL ethanol was prepared in a 250mL round-bottom flask with continuous magnetic stirring. Sulphur powder (0.3g) was added directly to the $HgCl_2$ solution and diluted to 200mL with ethanol. After 30 minutes of mixing, the round-bottom flask was placed in a sonication bath (Branson 5510, 185W). A borosilicate gas dispersion tube connected to nitrogen (< 1psi) was inserted to the bottom of the flask to generate a continuous flow of inert gas. After 30 minutes of sonication and purging, the sulphur powder began to disperse. A previously prepared NaOH solution (0.3g in 50mL ethanol using sonication to speed dissolution) was added dropwise via a peristaltic pump (1 drop·second^{-1}) to the $HgCl_2$ and sulphur mixture, while maintaining the nitrogen purge and sonication. As the base was added, the solution changed from yellow to orange and from orange to red and finally a black precipitate appeared. The final product was centrifuged at 4,193×g for 15 minutes and washed three times sequentially with ethanol, pentane and hexane. The entire synthesis procedure required 4-5 hours and yielded HgS NPs in a yield of approximately 70%. The product was collected and dried under nitrogen in a 60°C oven for three days before storage in an amber vial sealed with a cap, silicone-PTFE septum and nitrogen atmosphere. Samples removed from the sealed vials were analysed by TEM, XRD and XPS within 24 hours, since the oxidation of HgS is relatively slow [22].

In order to compare the effect of sonication and nitrogen purging on the NPs, these procedures were omitted in some batches. In these cases, mechanical shaking and magnetic stirring were used during NaOH addition and nitrogen was not used during mixing, reaction, or drying. The final products were compared by XRD and XPS.

2.2 Particle characterization techniques

An Hitachi 7600 TEM at 200kV accelerating voltage was used to image the nano β-HgS NPs. The samples were prepared in an absolute ethanol solution, deposited on a Cu grid with a carbon film and dried at 35°C overnight. XPS measurements to investigate the particle surface properties were performed on a Kratos Axis 16 spectrometer using monochromatic Al Kα radiation of 1486.6eV energy. C 1s at 284.8eV was used as the charge reference to determine the core level binding energies. For monitoring the hydrodynamic diameter of the aggregate and the optical band gap, a sample solution of 0.2 g·L^{-1} in water was sonicated for 30 minutes to reduce aggregation and then 1.5mL was transferred to a square cuvette. Each measurement was completed as quickly as

possible after sonication and was generally finished within 5 minutes. Hydrodynamic particle size distributions were determined by DLS using a Beckman-Coulter N4 Plus with a refractive index setting of 3.0 for software correction [23, 24]. The UV-visible absorbance spectra were determined on a Shimadzu UV-2501 PC. Luminescence spectra were acquired using a Photon Technology International QuantaMaster with excitation at 300nm and 6 and 1 nm bandpass on excitation and emission monochromators, respectively. Emission spectra were corrected for instrument responses. XRD patterns were obtained using a Scintag XDS 2000 (Cu-Kα, λ=1.5406 Å radiation, step scan mode, 0.05°/0.5 sec, 1 sec/step) over the range of 5° to 90°. Surface area was determined by the B.E.T. isotherm method on a Micromeritics ASAP 2010 Surface Area Analyser (N_2 adsorption).

3. Results and discussion

3.1 Particle characterization

The NPs synthesized with sonication and nitrogen gas purging were characterized with TEM, XRD, XPS, DLS, UV-vis spectroscopy. TEM images, as shown in Figure 1, indicate that the primary particles are of spherical shape with diameters of approximately 10-15nm. It is clear that primary particles interacted to form much larger aggregates. Figure 2 shows the distribution of the hydrodynamic diameters of the aggregates at approximately 200mg/L in water as measured with DLS. The histogram of the DLS results indicates that the primary particles aggregated irregularly, forming complex aggregates over a range of sizes. The average hydrodynamic diameter of the β-HgS aggregates determined in the triplicate measurements shown in Figure 2 is 296.2 ± 22.5nm. The range of aggregate sizes observed with TEM and DLS are generally consistent, with larger aggregates in TEM possibly formed during sample drying and preparation [25].

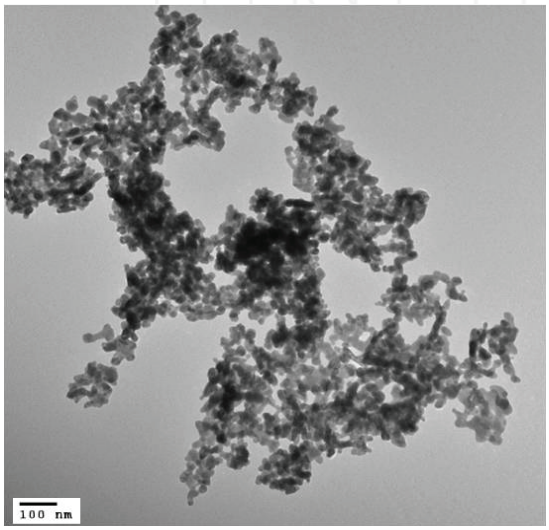

Figure 1. TEM image of β-HgS NPs with 100,000× magnification.

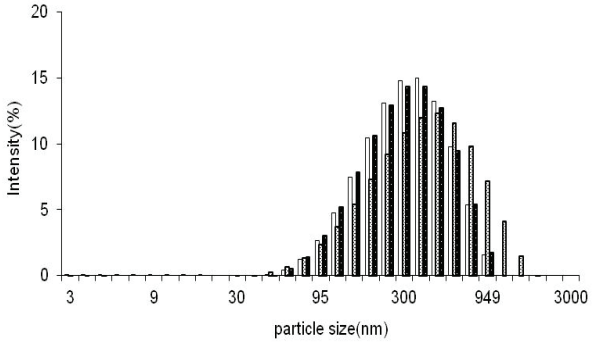

Figure 2. DLS results for β-HgS NP aggregate hydrodynamic diameter distribution (triplicate measurements) after 5 minutes of sonication.

The N_2 B.E.T. surface area result is 14.9 ± 0.2 $m^2 \cdot g^{-1}$. Assuming nonporous metacinnabar spheres of 7.7g/cm^3 density [26], this corresponds to average diameters of approximately 50nm. The measured surface area is 30% of the theoretical surface area of well-separated 15nm metacinnabar spheres. This comparison is also consistent with significant aggregation. In addition, sample drying prior to the N_2 B.E.T. measurement may contribute to aggregation [25].

The UV-visible absorbance and luminescence excitation and emission spectra of nano-sized β-HgS in ethanol are shown in Figure 3. A broad absorption peak with a local maximum at approximately 350 nm was observed and the excitation spectrum is consistent with this. The presence of aggregated particles contributed somewhat to background absorbance. Emission was observed in a relatively sharp peak near 425nm. This is comparable to results obtained for 20-40nm HgS nanoparticles formed in bovine serum albumin solutions by Qin et al. who observed an emission maximum at 440nm [27] and for 10-30nm HgS nanoparticles formed via dithiocarbamate complexes by Onwudiwe and Ajibade [28], who observed a maximum at 320nm. Sharp near-band-edge emission and the absorbance maximum are characteristic of nanoparticles with relatively narrow size distributions and flat, regular, defect-free surfaces that do not provide deep exciton traps [29, 30]. As shown in Figure 4, the bandgap (Eg) was calculated from the photon energy (E_{phot}) and the absorption coefficient (α) using a Tauc plot [31]. The band gap result is 2.3 eV, which indicates size quantization effects, changing the semi-metallic behaviour of bulk β-HgS (Eg=−0.5 eV) to semiconductor behaviour [20]. Table 1 shows a comparison of the particle sizes and bandgaps of β-HgS synthesized by different methods (two microwave, phase separation, electrochemical and this work). The particle diameters obtained using the hydrolysis approach of this work are intermediate, whereas the phase separation process gave the smallest diameters. The bandgap calculation results in Table 1 may be considered average values as they are based on the shape of the spectra, which is in turn

controlled by the particle size distribution. However, an analysis of the nanoparticle size distribution based on spectral features, such as that described by Pesika et al. [32], is not commonly performed or reported and therefore this comparison was not undertaken.

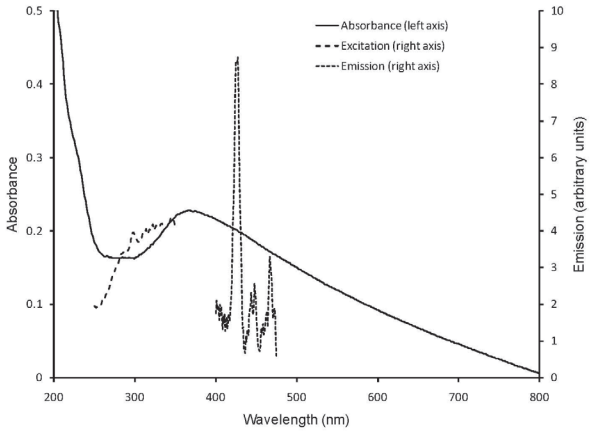

Figure 3. UV-visible absorbance (left axis) and luminescence excitation and emission (right axis) spectra of HgS NPs.

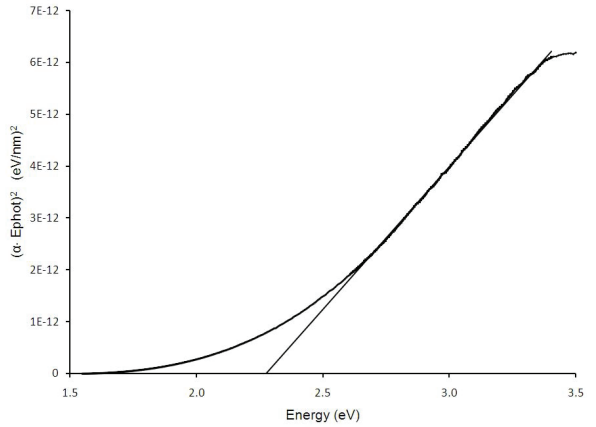

Figure 4. The energy Tauc plot of nHgS, where α is absorption coefficient and E_{phot} is photon energy.

Synthesis Method	Particle diameter (nm)	Bandgap (eV)
Microwave [17]	5-10	2.6
Microwave [16]	8-23	2.5
Phase separation [2]	1-5	1.5-2.1
Electrochemical [20]	15	1.4-2.0
This work	10-15	2.3

Table 1. Comparison of β-HgS NP size and bandgap

3.2 The influence of sonication

As described earlier, the effect of sonication was examined by using mechanical mixing methods only during synthesis. XRD spectra were obtained for β-HgS NPs generated by each synthesis procedure and used to compare crystal structure and particle size. Both treatments, with and without sonication, gave good agreement with the standard peaks and can be indexed as β-HgS with prominent crystallographic planes of (111), (200), (220) and (311), as shown in Figure 5. Note the full width at half the maximum (FWHM) of XRD peaks in sonicated samples is significantly broadened compared to unsonicated samples. Based on the Debye-Scherrer equation [33], for the (111) peak with 2θ at 26.2°, the average crystalline sizes of the β-HgS samples were approximately 11nm and 17nm for sonicated and unsonicated samples, respectively. Although the presence of nano-crystal defects and polycrystallinity may cause inaccurate estimations by the Debye-Scherrer equation [25], the repeated XRD analysis showed similar results with different batches of nanoHgS produced and the XRD particle size estimation is in good agreement with the TEM result. There are significant and reproducible size differences between sonicated and unsonicated samples, indicating that sonication is essential in the generation of smaller β-HgS particles.

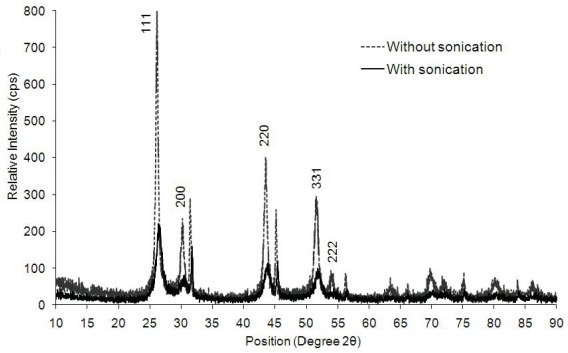

Figure 5. XRD patterns of nHgS from syntheses without (dashed line) and with (solid line) sonication.

3.3 The influence of nitrogen purging

During the synthesis of β-HgS NPs, nitrogen gas purging was used to prevent oxidation. The surface composition of nano β-HgS synthesized with and without nitrogen purging was studied by XPS, as shown in Figure 6.

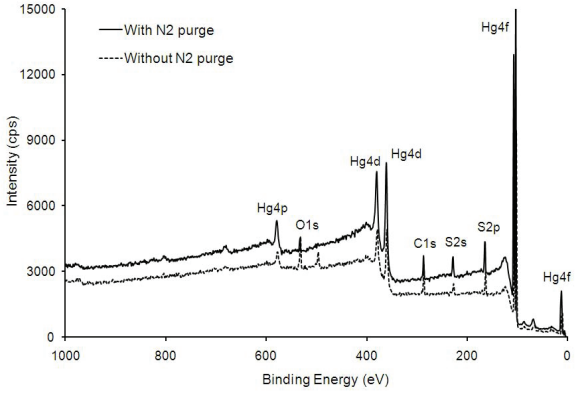

Figure 6. XPS spectra of β-HgS NPs with N_2 purge (solid line) and without N_2 purge (dashed line) during synthesis.

The energy axis was corrected by the C (1s) peak from 286-287eV to 284.6eV. All other peaks were corrected

accordingly, as shown in Tables 2 and 3, for quantification. Other than oxygen, no significant impurity peaks were detected, indicating that the products were of high purity. Nitrogen purging during synthesis significantly reduced the oxygen component from 24.8% to 6.1%. In addition, the atomic ratio of Hg (4f) to S (2p), 31:25, indicated that the surface of the product was slightly rich in mercury.

Peak	Position (eV)	Corrected position (eV)	Raw Area (CPS)	Atomic Conc %
O 1s	532	530.6	12234.7	24.83
C 1s	286	284.6	9258.3	49.77
S 2p	163	161.6	4294.4	9.57
Hg 4f	102	100.6	72400.0	15.83

Table 2. XPS analysis for β-HgS NPs without N_2 purge

Peak	Position (eV)	Corrected position (eV)	Raw Area (CPS)	Atomic Conc %
O 1s	533	530.6	2725.0	6.08
C 1s	287	284.6	6365.3	37.63
S 2p	165	162.6	10176.4	24.95
Hg 4f	103	100.6	130366.7	31.34

Table 3. XPS analysis for β-HgS NPs with N_2 purge

4. Mechanism of reaction

On the basis of these observations, a probable pathway for β-HgS formation is proposed. Mercuric chloride was dissolved in ethanol while elemental sulphur was partially dissolved and well dispersed. Upon addition of hydroxide, sulphur is known to hydrolyze to thiosulphate and polysulphides [34-35]. Consistent with reactions proposed by Li et al. [21], sulphide may be formed according to the reaction $3S + 6OH^- \rightarrow 2S^{2-} + SO_3^{2-} + 3H_2O$. As a base is gradually added under conditions of effective mixing and sonication, sulphide is produced and reacts with mercuric ions from the mercury salt to form β-HgS NPs. In the present work, the dominant effect of sonication appears to be dispersion of particles and aggregates to result in smaller nanoparticles, rather than driving reactions through heating or oxidation-reduction processes resulting from acoustic cavitations.

The colour changes observed in this work upon addition of hydroxide to the ethanolic solution of sulphur and mercuric ion (yellow to orange to red to black precipitate) may be compared to those described by Higginson et al. [2] and by Zhang et al. [36]. In the former, as bis(trimethylsilyl)sulphide is added to a reverse-micelle solution containing mercuric ions, colour changes from yellow through pink, purple, green and brown were observed and were shown to correspond to β-HgS NPs of increasing size. In the latter, the addition of elemental sulphur to ethylenediamine produced colour changes from green to yellow to colourless over a period of 20 hours and was attributed to polysulfide ions of decreasing size (S_6^{3-} and S_3^-). Both types of chemical changes could be occurring in the present work although differences in solvents and ligands could affect the absorbance of various species. Further detailed work is needed to identify the chemical species and to determine if it is possible to vary conditions in order to control NP sizes as achieved by Higginson et al. and the nanocrystalline phase as observed by Zhang et al.

5. Conclusion

The method to synthesize high purity β-HgS NPs from $HgCl_2$ and sulphur powder in ethanol is a simple and facile procedure. The sonication process improved the synthesis conditions and reduced the single particle diameter from 17nm to 11nm. The introduction of nitrogen purging during the synthesis and drying processes was performed to prevent oxygen contamination. This synthesis method is useful for generating uniform β-HgS NPs without the introduction of surfactants or toxic chemicals. The particle size, morphology, surface composition and surface area were characterized. In particular, aggregation is an important characterization of NP behaviour. The synthesized product contained few impurities. Based on comparison to other methods, the potential to further develop this approach to yield β-HgS and other metal chalcogenide NPs of controlled size and crystallinity exists.

6. Acknowledgments

The authors gratefully acknowledge support through Clemson University Public Service Activities and USDA Hatch project 1700399. The authors are also grateful to Dr. Don Vanderveer at Chemistry Department and staff at Electron Microscope Facility of Clemson University.

7. References

[1] Sapriel J (1971) Cinnabar (α HgS), a Promising Acousto-Optical Material. Appl. Phys. Lett. 19: 533-535.

[2] Higginson KA, Kuno M, Bonevich J, Qadri SB, Yousuf M, Mattoussi H (2002) Synthesis and Characterization of Colloidal β-HgS Quantum Dots. J. Phys. Chem. B 106: 9982-9985.

[3] Chakraborty I, Mitra D, Moulik SP (2005) Spectroscopic Studies on Nanodispersions of CdS, HgS, their Core-shells and Composites Prepared in Micellar Medium. J. Nanopart. Res. 7: 227-236.

[4] Kershaw SV, Harrison M, Rogach AL, Kornowski A (2000) Development of IR-Emitting Colloidal II–VI Quantum-Dot Materials. IEEE J. Sel. Top. Quantum Electron. 6: 534-543.

[5] Roberts GG, Lind EL, Davis EA (1969) Photoelectronic Properties of Synthetic Mercury Sulphide Crystals. J. Phys. Chem. Solids. 30: 833-844.

[6] Virot F, Hayn R, Richter M, van den Brink J (2011) Metacinnabar (β-HgS): A Strong 3D Topological

Insulator with Highly Anisotropic Surface States J, Phys. Review Letter. 106: 236806-1-4.
[7] Barnett MO, Harris LA, Turner RR, Stevenson RJ, Henson TJ, Melton RC, Hoffman DP (1997) Formation of Mercuric Sulfide in Soil. Environ. Sci. Technol. 31: 3037-3043.
[8] Gerbig CA, Kim CS, Stegemeier JP, Ryan JN, Aiken GR (2011) Formation of Nanocolloidal Metacinnabar in Mercury-DOM-Sulfide Systems. Environ. Sci. Technol. 45: 9180-9187.
[9] Deonarine A, Hsu-Kim H (2009) Precipitation of Mercuric Sulfide Nanoparticles in NOM-Containing Water : Implications for the Natural Environment. Environ. Sci. Technol. 43: 368-2373.
[10] Graham AM, Aiken GR, Gilmour CC (2012) Dissolved organic matter enhances microbial mercury methylation under sulfidic conditions. Environ. Sci. Technol. 46: 2715-2723.
[11] Zhang T, Kim B, Levard C, Reinsch BC, Lowry GV, Deshusses MA, Hsu-Kim H (2012) Methylation of Mercury by Bacteria Exposed to Dissolved Nanoparticulate, and Microparticulate Mercuric Sulfides. Environ. Sci. Technol. 46: 6950-6958.
[12] Kale SS, Lokhande CD (1999) Preparation and Characterization of HgS Films by Chemical Deposition. Mater. Chem. Phys. 59: 242-246.
[13] Zeng J, Yang J, Qian Y (2001) A Novel Morphology Controllable Preparation Method to HgS. Mater. Res. Bull. 36: 343-348.
[14] Qin A, Fang Y, Zhao W, Liu H, Su C (2005) Directionally Dendritic Growth of Metal Chalcogenide Crystals via Mild Template-free Solvothermal Method. J. Cryst. Growth. 283: 230-241.
[15] Liao X H, Zhu JJ, Chen HY (2001) Microwave Synthesis of Nanocrystalline Metal Sulfides in Formaldehyde Solution. Mater. Sci. Eng. B B85: 85-89.
[16] Wang H, Zhang JR, Zhu JJ (2001) A Microwave Assisted Heating Method for the Rapid Synthesis of Sphalrite-Type Mercury Sulfide Nanocrystals with Different sizes. J. Cryst. Growth. 233: 829–831.
[17] Ding T, Zhu J (2003) Microwave Heating Synthesis of HgS and PbS Nanocrystals in Ethanol Solvent. Mater. Sci. Eng. B. 100: 307-313.
[18] Ren T, Xu S, Zhao W, Zhu J (2005) A Surfactant-Assisted Photochemical Route to Single Crystalline HgS Nanotubes. J. Photochem. Photobiol. A 173: 93-98.
[19] Mahapatra AK, Dash AK (2006) α-HgS Nanocrystals: Synthesis, Structure and Optical Properties. Physica E. 35: 9-15.
[20] Patel BK, Rath S, Sarangi SN, Sahu SN (2007) HgS Nanoparticles: Structure and Optical Properties. Appl. Phys. A 86: 447-450.
[21] Li Y, Ding Y, Liao H, Qian Y (1999) Room-Temperature Conversion Route to Nanocrystalline Mercury Chalcogenides HgE (E=S,Se,Te). J. Phys. Chem. Solids 60: 965-968.
[22] Hsu-Kim H, Sedlak DL (2005) Similarities between Inorganic Sulfide and the Strong Hg(II)-Complexing Ligands in Municipal Wastewater Effluent. Environ. Sci. Technol. 39: 4035-4041.
[23] Palik ED (1998) Handbook of Optical Constants of Solids, 2nd ed. Academic Press, New York.
[24] Murdock RC, Stolle LB, Schrand AM (2008) Characterization of Nanomaterial Dispersion in Solution Prior to In Vitro Exposure Using Dynamic Light Scattering Technique.
[25] Jeong HY, Lee JH, Hayes KF (2008) Characterization of Synthetic Nanocrystalline Machinawite : Crystal Structure, Particle Size and Specific Surface Area. Geochim Cosmochim AC72: 493-505.
[26] Haynes WM (2012) CRC Handbook of Chemistry and Physics, 92nd ed.(Internet Version 2012), CRC Press/Taylor and Francis, Boca Raton, FL.
[27] Qin DZ, Ma XM, Yang L, Zhang L, Ma ZJ, Zhang J (2008) Biomimetic Synthesis of HgS Nanoparticles in Bovine Serum Albumin Solution. J. Nanopart. Res. 10: 559-566.
[28] Onwudiwe DC, Ajibade PA (2011) ZnS, CdS and HgS Nanoparticles via Alkyl-Phenyl Dithiocarbamate Complexes as Single Source Precursors. Int. J. Mol. Sci. 12 :5538-5551.
[29] Landes CF, Braun M, El-Sayed MA (2001) On the Nanoparticle to Molecular Size Transition : Fluorescence Quenching Studies. J. Phys. Chem. B. 105 :10554-10558.
[30] Murray CB, Norris DJ, Bawendi, MG (1993) Synthesis and Characterization of Nearly Monodisperse CdE (E=S,Se,Te) Semiconductor Nanocrystallites. J. Amer. Chem. Soc. 115 :8706-8715.
[31] Tsunekawa S, Fukuda T (2000) Blue Shift in Ultra-violet Absorption Spectra of Monodisperse CeO_{2-X} Nanoparticles. J. Appl. Phys. 87: 1318-1321.
[32] Pesika NS, Stebe KJ, Searson PC (2003) Relationship between Absorbance Spectra and Particle Size Distributions for Quantum-Sized Nanocrystals. J. Phys. Chem, B 107: 10412-10415.
[33] Warren BE (1969) X-Ray Diffraction, Addison-Wesley, Massachusetts.
[34] Parker AJ, Kharasch N (1959) The Scission of the Sulfur-Sulfur Bond. Chem. Rev. 59: 583-628.
[35] Foss O (1959) The Ionic Scission of the S-S Bond. In: Organic Sulfur Compounds, Vol. I. Pergamon Press, London.
[36] Zhang J, Chen Z, Wang Z, Ming N (2004) The Synthesis of HgS Microcrystallites with Controllable Structure and Morphology. Mater. Res. Bull. 39: 2241-224.